LAWRENCE
LIVERMORE
NATIONAL
LABORATORY

LLNL-PROC-661274

In situ neutron diffraction study of the deformation mechanisms in solutionized Mg-Zn alloys

R. P. Mulay, C. Caceres, S. R. Agnew

September 24, 2014

TMS 2015
Orlando, FL, United States
March 15, 2015 through March 19, 2015

Disclaimer

This document was prepared as an account of work sponsored by an agency of the United States government. Neither the United States government nor Lawrence Livermore National Security, LLC, nor any of their employees makes any warranty, expressed or implied, or assumes any legal liability or responsibility for the accuracy, completeness, or usefulness of any information, apparatus, product, or process disclosed, or represents that its use would not infringe privately owned rights. Reference herein to any specific commercial product, process, or service by trade name, trademark, manufacturer, or otherwise does not necessarily constitute or imply its endorsement, recommendation, or favoring by the United States government or Lawrence Livermore National Security, LLC. The views and opinions of authors expressed herein do not necessarily state or reflect those of the United States government or Lawrence Livermore National Security, LLC, and shall not be used for advertising or product endorsement purposes.

In-situ neutron diffraction study of the deformation mechanisms in solutionized Mg-Zn alloys

R. P. Mulay[1], S.R. Agnew[2] and C. H. Caceres[3]

[1] Lawrence Livermore National Laboratories, Livermore, California, 94550, USA

[2] Department of Materials Science and Engineering, University of Virginia, Charlottesville, VA 22904-4745, USA

[3] Materials Engineering, School of Engineering, University of Queensland Brisbane, Queensland 4072, Australia

Keywords: neutron diffraction, solid solution strengthening, magnesium, elastic strains

Abstract

In-situ neutron diffraction experiments were carried out on solutionized and randomly textured Mg-Zn alloy castings with similar grain sizes but variation in Zn content from 1.7 to 6.6 wt %. The evolution in internal elastic strains and diffraction peak intensities with increasing load were analyzed. The macroscopic stress strain curve shows an increase in yield strength with an increase in zinc content. Neutron diffraction results indicate that the strength of basal slip, tension twinning and <c+a> slip/compression twinning modes increases with increase in zinc content. However, the strength of prismatic slip appears to be unaffected by zinc content at lower concentrations and increases with zinc content only at higher concentrations. These results are discussed in light of prior work on the Mg-Zn system.

Introduction

There is a great interest in the use of magnesium alloys as structural materials due to their low density. Efforts are being made to increase the strength of magnesium alloys through solid solution strengthening and age hardening [1,2,3]. Several studies have examined the deformation mechanisms in magnesium. The primary deformation mechanisms active at room temperature are basal slip, prismatic slip and tension twinning [4]. Single crystal studies have shown that basal slip is the softest deformation mechanism [5]. However, studies on polycrystalline samples have shown that the activation of tension twinning or prismatic slip are necessary for macroscopic yielding to occur [6,7].

Single crystal studies have shown that the prismatic slip mode softens with the addition of common alloying elements, such as Al and Zn [8]. However, basal slip shows the conventional solid solution strengthening effect [9]. Prior work on polycrystalline Mg-Zn alloys with concentrations ranging from 0 to 6.6 wt % Zn suggest that solid solution softening of the prism planes can reduce the yield strength for concentrations up to 1.7 wt% Zn. Beyond this concentration the softening effects are offset by the overall solid solution hardening effects [10]. However, effects of twinning were not considered in that study. Recently, Stanford and Barnett [11] examined textured Mg-Zn alloys in the concentration range 0 to 2.8 wt % Zn under deformation conditions designed to favor a certain deformation mode. They found that the critical resolved shear stress (CRSS) for twinning was not affected by zinc content while that of basal slip increased with increase in zinc content. In case of prismatic slip they found solid solution softening to be present only above grain sizes of ~ 50 um.

The present work examines the effect of Zn additions in the range of 1.7 to 6.6 wt % on the deformation mechanisms in solutionized Mg-Zn alloys using in-situ neutron diffraction. The experiments are done on cast Mg-Zn alloys with a weak (essentially random) initial texture.

Experimental Procedure

Material

Mg-Zn castings with nominal compositions of around 1.5 to 6.5 wt % Zn were made by melting commercially pure Mg (99.7 wt%) and Zn using an electrical resistance furnace in small boron nitride coated steel crucibles. Grain refinement was carried out by using a Mg–Zr master alloy (77 wt % Mg and 23 wt % Zr). An atmosphere of 0.5%SF_6 in dry air was used to protect the molten alloy from oxidation. Alloying additions were made at 700 °C. The melt was then mixed with a mechanical stirrer for 15 minutes and subsequently poured into split steel moulds preheated to 200 °C under protective atmosphere. The cast cylinders were 90 mm in height, 50 mm in diameter.

The cast cylinders were then sectioned in half, solution heat treated under nitrogen atmosphere and quenched into water. The actual compositions were determined using inductively coupled plasma-atomic emission spectroscopy (ICP-AES) [10, 12] and are listed in Table 1. In this paper, the alloys are referred to by their determined composition in wt% Zn. For each composition a longitudinal section was mechanically polished down to 1 μm and then etched with acetic-picral acid. The grain size was subsequently determined using the linear intercept method according to ASTM E112-88 and at least 300 intercepts were counted. The grain sizes are listed in Table 1. More details of the casting, heat treatment and grain size measurement procedures can be found elsewhere [10,12]. The castings used in this study are from the same batch used in references 10 and 12. All three compositions have similar grain sizes (within a factor of 2). Metallographic examination of the samples showed that they were single phase [12]. Cylinders 20 mm in length and 10 mm in diameter were machined from the castings for in-situ testing.

Table 1: Compositions (determined by ICP-AES) and grain sizes of the Mg-Zn alloys examined

Zn (wt %)	Zn (at.%)	Zr (wt %)	Zr (at.%)	Grain size (μm)
1.7	0.64	0.22	0.06	61
4.1	1.56	0.51	0.14	38
6.6	2.59	0.54	0.15	41

Initial texture measurements

Prior to compression testing, the initial texture was measured using the HIgh-Pressure Preferred Orientation diffractometer (HIPPO), at the Manuel Lujan Jr. Neutron Scattering Center (LANSCE, Los Alamos, NM). HIPPO allows for rapid characterization of full orientation distributions of bulk samples and has been designed to optimize the collection of texture data through the use of high neutron intensities and a large number of time of flight detectors. Since this is a neutron diffraction based method, it is not surface limited like X-rays or electron based techniques. A full description of HIPPO can be found elsewhere [13].

Compression testing

The compression tests were performed on a custom built Instron (Norwood, MA) load frame in the flight path of the time-of-flight neutron beam line, Spectrometer for MAterials Research at Temperature and Stress (SMARTS), at the Manuel Lujan Jr. Neutron Scattering Center (LANSCE, Los Alamos, NM). The tests were carried out at room temperature in position control at a constant velocity 0.01 mm/s which corresponds to an initial strain rate of 5×10^{-4}/s. An extensometer was attached to the sample using rubber bands to measure the strain. The compression axis was aligned with the cylindrical axis of the samples. The samples were lubricated using molybdenum disulfide (MoS_2) grease. One sample of each composition was tested due to the time limitations on the neutron beam line.

In-situ neutron diffraction

A detailed description of SMARTS is given elsewhere [14]. A short description is provided here. The loading axis is oriented at 45° relative to the incident neutron beam. Two detector banks are situated at ±90°, making it possible to simultaneously collect two complete diffraction patterns, one parallel and one perpendicular to the applied load. Since the in-situ testing setup is horizontal, the compression sample was preloaded to a stress of ~5 MPa. The initial d_0^{hkl} spacing measured at ~5 MPa is considered to be the ‘‘stress-free’’ spacing. The neutron diffraction measurements were carried out at several points along the stress-strain curve. The load frame was held at a constant position during diffraction pattern collection, and the hold time was varied to obtain a constant neutron count at the detectors (governed by the source current and the material neutron absorption and scattering cross sections). For this material, the collection time is approximately 10 to 12 minutes per pattern.

Internal strains within grains that satisfy the Bragg condition for a given {hkl} reflection are calculated from the difference between the measured and stress-free lattice spacing,

$$\varepsilon^{hkl} = \frac{d^{hkl} - d_0^{hkl}}{d_0^{hkl}}$$

where d_0^{hkl} is the stress free lattice spacing and d^{hkl} is the measured lattice spacing. The peak shifts and corresponding internal elastic strains were then calculated using single peak fits with an instrument specific code developed at LANSCE [15] which uses the General Structural Analysis System (GSAS) [16].

Results

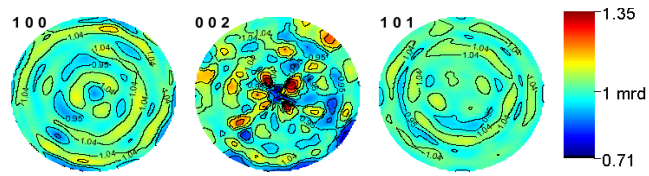

Figure 1: Pole figures showing the initial texture measured for the Mg-1.7 wt % Zn sample. The cylindrical axis of the sample is pointing out of the paper. The texture is essentially random.

The initial texture measured in the Mg-1.7 wt % Zn sample is shown in Figure 1. Similar textures were observed in case of the other two compositions examined in this study. The texture was very weak (essentially random) and axisymmetric. The cylindrical axis of the sample is pointing out of the paper.

Figure 2 shows the stress-strain curves obtained for the three zinc concentrations tested. The rubber bands holding the extensometer broke in the middle of the test in case of the 6.6 wt % Zn sample and hence extensometer strain data is not available for this sample. Thus, the strain plotted in Figure 2 has been calculated from the crosshead displacement to enable equitable comparison of all three samples. Strain obtained from extensometer measurements for the 1.7 and 4.1 wt % Zn samples has been shown in Figure 4a and 4b respectively. The macroscopic yield point (0.2 % strain offset) increases with increase in zinc concentration as seen in Figure 2. The yield point is ~55 MPa for the 1.7 wt % Zn sample, ~80 MPa for the 4.1 wt % Zn sample and ~92.5 MPa for the 6.6 wt % Zn sample. The strain hardening rate appears to be similar in all three samples. None of the samples were strained to failure. The load drops in the stress-strain curves correspond to the points where the test was stopped and held and a constant position to collect neutron diffraction patterns.

Figure 3 shows a diffraction pattern obtained from the 6.6 wt % Zn sample in the stress free condition parallel to the loading axis. No second phase peaks were present in any of the diffraction patterns suggesting that the samples were in the solutionized condition, though it must be admitted that this diffraction technique is not sensitive to very small volume fractions of second phase particles. The diffraction patterns obtained from all three concentrations examined were similar.

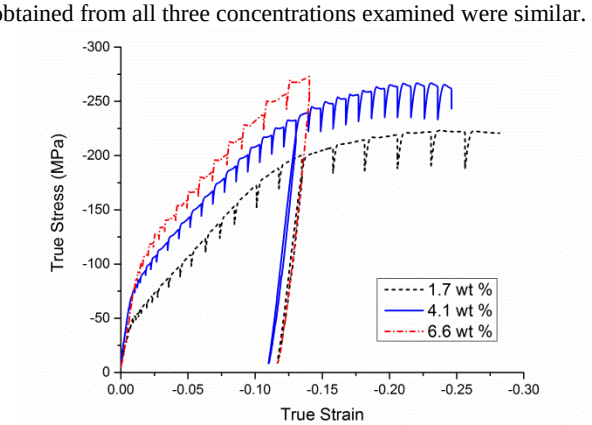

Figure 2: Stress- strain curves obtained from the Mg-Zn alloys. The load drops correspond to the points where diffraction data was collected by holding the test at a constant position.

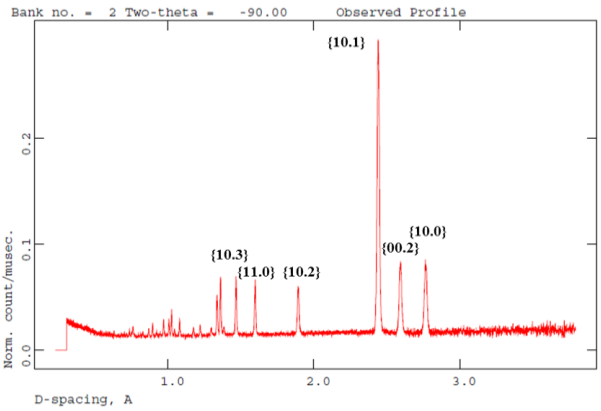

Figure 3: Diffraction pattern obtained from the 6.6 wt % Zn sample in the stress free condition from the bank parallel to the loading axis. No second phase peaks are present.

Figure 4 shows the stress-strain curves, the internal strains and peak intensity evolution from the 1.7, 4.1 and 6.6 wt % Zn samples respectively. As mentioned above, in the case of the 6.6 wt % Zn sample strain has been calculated from crosshead displacement. In Figure 4 c the apparent elastic strain has been subtracted and only the true plastic strain has been plotted. Consider the 1.7 wt % Zn sample first. Initially the internal strains in all the sets of grains increase at the same rate, which is reflective of the elastic isotropy in Mg. Past the micro-yield point (20-25 MPa) (Fig. 4a) there is a bifurcation in the internal strains. The {10.2} (ideally oriented for basal slip) and {10.1} (also well oriented for basal slip) diverge to the left, indicating these sets of grains have yielded and reduce their share of elastic strains. This suggests that the critical resolved shear stress (CRSS) is approximately 10 MPa in this dilute Mg-Zn alloy. On the other hand, the {11.0} and {00.2} sets of grains that diverge to the right are still accommodating most of the strain elastically. Hence, they must start sharing a greater amount of the elastic strain. If one could average the lattice strains in all grains, the result would correspond to Hooke's law (i.e. a linear relation between the applied stress and the average lattice strain with slope equal to Young's modulus).

The next inflection occurs at an applied stress of approximately 40 MPa, which is close to the macroscopic yield point (~55 MPa). At this point, the {11.0} grains and {00.2} grains diverge. A simple Schmid analysis (which must be applied with caution, given the fact that stresses are non-uniform among the grains at this stage) shows that this could be due to the activation of non – basal (prismatic) slip or tensile twinning [17], provided a CRSS of about 20 MPa. Distinction between the two modes can be made by observing peak intensity changes. From figure 4a (right hand side) it can be seen that, beyond this stress level, the intensity of the {00.2} reflection starts increasing rapidly and that of the {11.0} starts decreasing. The {10.1} and {10.2} intensities exhibit less rapid change. This type of texture evolution is a signature of tension twinning (whereby grains most favorably oriented for twinning, with c-axes perpendicular to the compression axis, are reoriented by nearly 90° to closely align with the compression axis).

At an applied stress of 135-140 MPa, the lattice strain evolution in the {11.0} grains slows. This indicates that the prismatic slip system has become active in this material. With such widely varying internal strain levels in the grains, it would be unwise to speculate too confidently about the CRSS value for prismatic slip without employing a polycrystal plasticity model, however, it is certainly higher than that of twinning and would appear to be in the vicinity of 60 MPa, given the fact that the lattice strain level in the {11.0} grains does not depart far from a linear extrapolation of the internal strain evolution during the elastic region and the Schmid factor for prismatic slip in {11.0} grains is m = 0.43.

At higher stress levels, the only significant inflection of note is the gradual bending of the {00.2} lattice strain curve at an applied stress which corresponds with the point where the linear hardening behavior gives way to a decreasing strain hardening rate and, finally, saturation of the flow curve (beginning at about 150 MPa). This could be because the grains have essentially exhausted the twinning mechanism reflected by the fact that the intensity of the {00.2} reflection is only increasing slowly. This twinning has placed a significant volume fraction of grains in a hard orientation (c-axes parallel to the compression axis), which can only be relaxed by <c+a> slip or compression twinning [6, 7]. Saturation of the flow curve at 225 MPa is probably reflective of the activity of one or more of these hard modes.

Similar observations can be made in the sample with 4.1 wt % Zn. The difference is that in this sample these inflections occur at higher stress (Fig. 4 b). Microyielding of the {10.2} grains occurs at approximately 45 MPa and the macroscopic yield point beyond which twinning is active occurs around 70 MPa. This suggests that there is solid solution hardening of both the basal slip (CRSS of about 20 MPa) and tension twinning deformation modes. It is admitted that the effect on twinning could be secondary, given the fact that nucleation of twinning is generally associated with stress concentrations related to basal slip [e.g.18]. The prismatic slip mode again appears to have been activated at an applied stress level of 140 MPa. Again, this suggests a CRSS value in the vicinity of 60 MPa, which indicates that prismatic slip is neither radically hardened nor softened in this range of solute addition. Finally, the linear strain hardening behavior terminates at around 175 MPa, and saturation occurs at 270 MPa. This suggests that the <c+a> and/or compression twinning modes are solution strengthened.

For the highest concentration sample examined in this study (6.6. wt % Zn, shown in Fig. 4 c), the {10.2} grains, favorably oriented for basal slip, appear to yield at 60 MPa, suggesting a CRSS of 30 MPa. The second inflection occurs quickly thereafter, ~75 MPa, at which point the tensile twinning mode appears to have been activated, given the onset of rapid intensity changes in the {00.2} and {11.0} peaks, in particular. The next inflection in the internal strain development of {11.0} grains again suggests activation of prismatic slip. This time it occurs at around 170 MPa. This suggests that either solid solution strengthening has finally set in, or precipitation at a level insufficient to be observed by neutron diffraction has begun to influence the activity of prismatic slip. In this final test, the flow curve never saturates and the internal strain evolution in the {00.2} grains has not slowed, even at 275 MPa. This suggests that the <c+a> and/or compression twinning modes continue to be hardened by the additional alloy content.

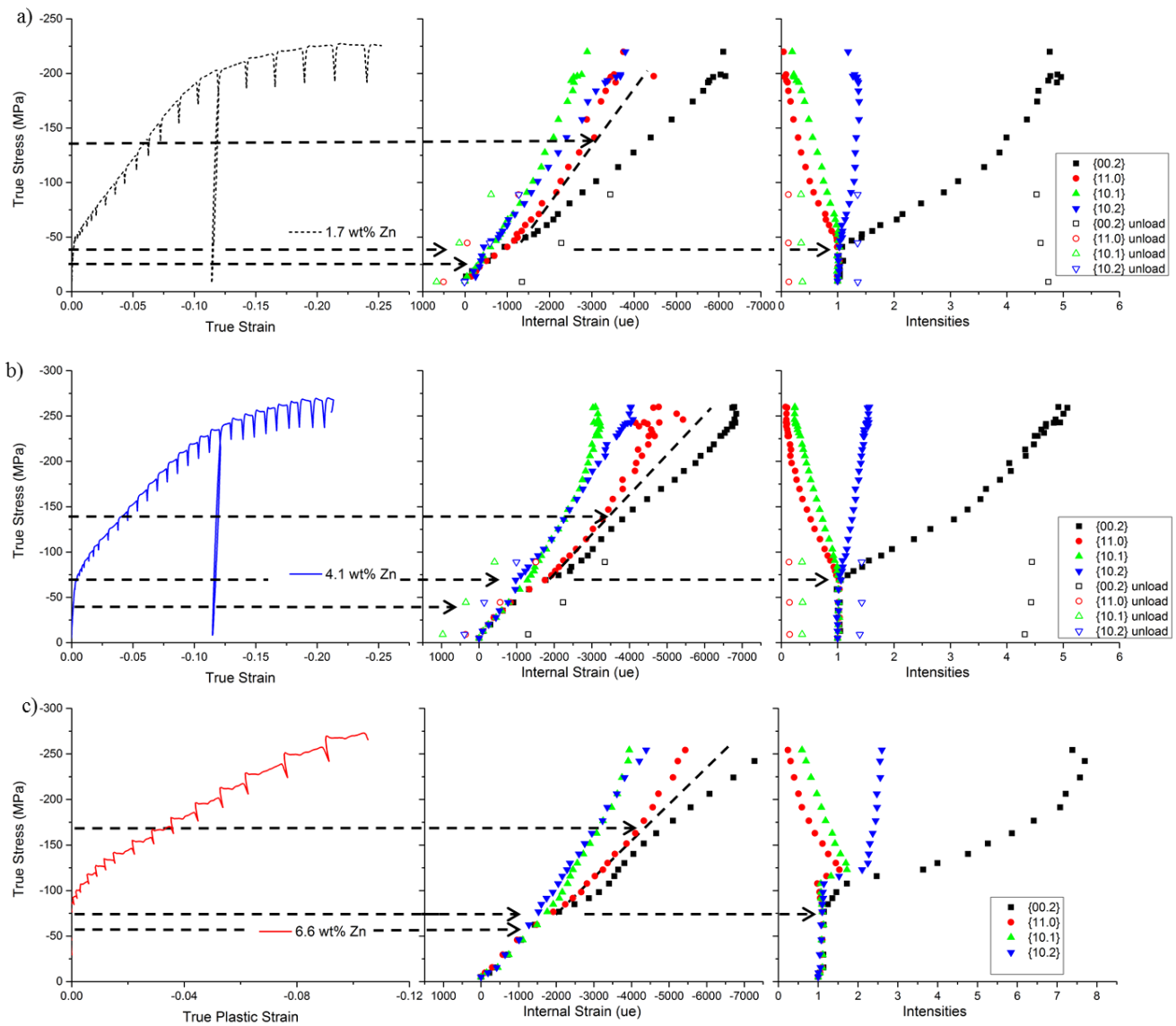

Figure 4: Stress-strain, internal elastic strains and diffraction peak intensity evolution for a) 1.7 b) 4.1 and c) 6.6 wt % Zn samples. The arrows are indicative of points where transitions are taking place.

The initial texture is essentially axisymmetric (since it is near random for all three samples) and since the compression process is inherently axisymmetric, it is possible to reconstruct the full texture at every point along the stress-strain curve where diffraction data is collected from the two diffraction patterns measured using SMARTS. Figure 5 shows the evolution of the axial distribution of the {00.2} poles as multiples of random distribution (MRD) with increasing stress in the 1.7 wt % Zn sample. Similar results were obtained for the 4.1 and 6.6 wt % samples. The intensity of the {00.2} peak increases significantly near the compression axis and reduces perpendicular to the compression axis. Assuming that the evolution of the {00.2} peak intensity is primarily due to deformation twinning (i.e., ignoring the rotations due to slip), it is possible to estimate the volume fraction of twinning as a function of deformation. The following relationship was employed,

$$f_{tw} = \int_0^{48} \{I(\chi) - I_0(\chi)\} \sin\chi d\chi$$

where χ is the angle of tilt between the {00.2} poles and the compressions axis and $I(\chi)$ is the intensity of the distribution at that tilt angle. If $I(\chi)\sin\chi$ is integrated from 0-90° the result will always be 1. A similar method was employed in previous work [17,19]. In the present case, we subtract the initial angular distribution $I_0(\chi)\sin\chi$, since we are interested in the change in intensity and not the absolute values. In the present work, the intensity of the axial distributions was equal around 48°, i.e., the volume fraction of grains with this orientation neither increase nor decrease. Hence, this angle was selected as the angle dividing regions associated with parents and twins. Figure 6 shows the twin volume fractions plotted as a function of stress for the three samples examined in this study. It can be seen that as the concentration of zinc increases, the stress necessary to produce the

same volume fraction of twins increases. This observation is consistent with the observations made from the internal strains where a higher stress was found necessary to activate twinning with increase in zinc concentration.

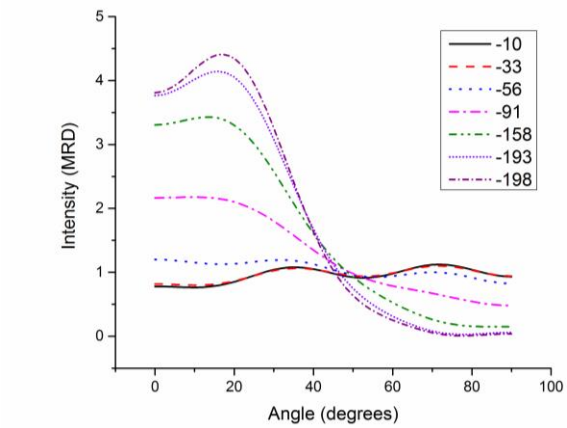

Figure 5: Axial distibution of the {00.2} poles in the 1.7 wt % Zn sample with increasing stress (MPa). The angles are measured with respect to the compression axis. There is a large evolution in the intensity of the {00.2} peak which is used to determine the amount of deformation twinning.

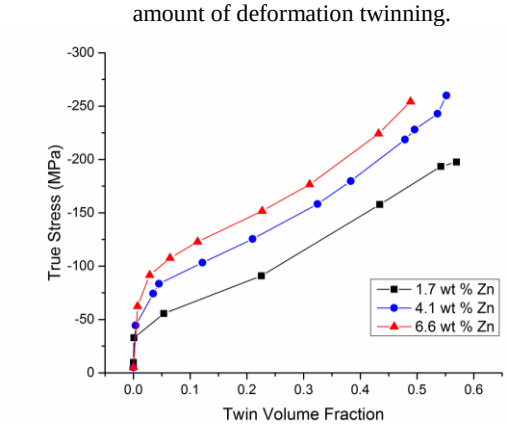

Figure 6: Twin volume fraction as a function of stress in 1.7, 4.1 and 6.6 wt % Zn samples.

A final point about the intensity evolution for the highest Zn content sample, shown in Fig. 4 c, is in order. Note that the relative intensity of all peaks suddenly increase at around 100 MPa. This is not indicative of a change in texture, since that would require some peaks to loose intensity. Because texture evolution is used as a fingerprint of twin activation, understanding the fundamental cause of this intensity change is of interest. However, no satisfying explanation has been forthcoming, as of yet. The aforementioned approach to estimating twin volume fraction is based upon a direct assessment of the texture evolution itself. The fact that the texture evolution is continuous (see Fig. 6) through the region where the discontinuity in the intensity is observed gives some confidence that there some other experimental artifact is responsible.

Discussion

The CRSS value of the basal slip mode is found to increase with an increase in zinc concentration from about 10 MPa for 1.7 wt % Zn to 30 MPa for 6.6 wt % Zn (Table 2). Without employing crystal plasticity modeling, the uncertainty in these estimates is nearly 5 MPa, so further work is planned. That said, prior work on Mg-Zn single crystals [9] and highly textured polycrystalline alloys [11] have shown a similar trend for concentrations up to 2.8 wt % Zn. While the estimated values of the CRSS are higher than those measured in the case of the single crystals (~ 1 MPa) [8,9], the current values show a continued solid solution strengthening trend even at higher Zn concentrations than those characterized in those original studies. Further, the CRSS values are in the same range as those obtained in a recent study of textured polycrystals favoring basal slip for samples with similar grain sizes [11]. Recent polycrystal plasticity modeling work [20, 21] on alloys similar to the present study (i.e., randomly textured cast alloys with a composition range of 0 to 6.6 wt % Zn) predicted a similar trend in the CRSS values.

Table 2: CRSS values (MPa) estimated for the different deformation modes based upon internal strain measurements.

	Basal slip	Tension twinning	Prismatic Slip
1.7 wt % Zn	10	20	60
4.1 wt % Zn	20	35	60
6.6 wt % Zn	30	38	75

The CRSS for twinning was also found to increase with increase in Zn content, from 20 to 38 MPa (Table 2). Also, the stress necessary to produce the same volume fraction of twins was found to increase with increase in zinc content (Fig. 6). Prior work on Mg single crystals found the CRSS for twinning to be independent of zinc concentration in the range examined (up to 2.8 wt % Zn) [5]. Stanford and Barnett [11] also found that the CRSS for twinning was ~15 MPa for a grain size of ~40 um irrespective of the Zn concentration. However, these samples were strongly textured. As multiple deformation mechanisms are necessary for yielding in randomly textured polycrystals, it is possible that the increase seen in the current work is a result of the increase in CRSS of basal slip. However, polycrystal plasticity modeling work carried out by Raeisinia and Agnew on randomly textured cast alloys [21] also showed an increase in twinning stress with zinc concentration up to around 2.1 wt % Zn followed by a saturation or slight decrease in CRSS. However, there was sufficiently large scatter in the data which precludes drawing firm conclusions. Again, it is admitted that the effect of Zn solute on twinning in these randomly textured castings is distinct from the insensitivity reported recently, based upon studies of textured samples [11]. Further work is planned involving crystal plasticity modeling of the results in order to lower the uncertainly levels in the estimates of the CRSS values of all the individual deformation mechanisms.

The CRSS of the prismatic slip mode seems to be unaffected by zinc content in the lower concentration range examined in this study and finally appears to increase with an increase in zinc content. Work carried out on single crystal Mg-Zn alloys [8] with zinc concentrations up to 1.1 wt % zinc showed a decrease in CRSS of the prismatic slip mode, especially at low temperatures. Stanford and Barnett observed a decrease in the CRSS value only in samples with grain sizes larger than 50um and in the concentration range of 0-1.1 wt % Zn [11]. In the range of 1.1 to 2.8 wt % Zn the CRSS values were independent of concentration for all grain sizes examined. Raeisinia et al. [20], in their reanalysis of early single crystal data [8,9], also showed that the CRSS of the prismatic slip mode is largely unaffected by zinc concentrations above ~1.1 wt % Zn. In the present work, all

samples have concentrations above 1.1 wt % Zn, which explains the relative independence of the CRSS on zinc concentration. The increase in CRSS observed in the 6.6 wt % sample is indicative of either solid solution hardening setting in or precipitation beginning to occur which cannot be detected by neutron diffraction.

Finally, the present work provides some insight into the effect of zinc content on the stress necessary to activate the hard modes of <c+a> slip and / compression twinning. The stress necessary to activate these modes appears to increase with an increase in the zinc content.

Conclusions

Solutionized Mg-Zn alloys with zinc content from 1.7 to 6.6 wt % were examined. The macroscopic yield point was found to increase with increase in zinc concentration. In-situ neutron diffraction results revealed that the strength necessary to activate basal slip, tension twinning and <c+a> slip/compression twinning modes all increased with an increase in zinc content. On the other hand, the stress necessary to activate prismatic slip is unaffected at lower concentrations of zinc but increases at higher concentrations. Similar to recent findings obtained from studies of textured polycrystals [11], no solute softening of the prismatic slip mode was observed.

Acknowledgements

A portion of this work was performed under the auspices of the U.S. Department of Energy by Lawrence Livermore National Laboratory under Contract DE-AC52-07NA27344 and has been assigned the document release ID #LLNL-PROC-661274.This work has benefited from the use of the Lujan Neutron Scattering Center at LANSCE, funded by the Department of Energy's Office of Basic Energy Sciences. Los Alamos National Laboratory is operated by Los Alamos National Security LLC under DOE Contract DE-AC52-06NA25396. The assistance of Lujan Center researchers D.W. Brown and B. Clausen is gratefully acknowledged.

References

1. J. B. Clark, "Age hardening in a Mg-9 wt.% Al alloy," *Acta Metallurgica*, 16(2) (1968), 141-152.
2. L. Gao, R. S. Chen, and E. H. Han, "Solid solution strengthening behaviors in binary Mg–Y single phase alloys," *Journal of Alloys and Compounds*, 472(1) (2009), 234-240.
3. J. B. Clark, "Transmission electron microscopy study of age hardening in a Mg-5 wt.% Zn alloy," *Acta Metallurgica*, 13(12) (1965), 1281-1289.
4. A. V. Beck, ed., *The technology of magnesium and its alloys* (London: FA Hughes & Co Ltd, 1943)
5. E. W. Kelley, and W. F. Hosford JR, "Plane-strain compression of magnesium and magnesium alloy crystals," *Trans Met Soc AIME*, 242(1) (1968), 5-13.
6. S. R. Agnew, D. W. Brown, and C. N. Tomé, "Validating a polycrystal model for the elastoplastic response of magnesium alloy AZ31 using in situ neutron diffraction," *Acta materialia*, 54(18) (2006), 4841-4852.
7. S. R. Agnew, et al., "Study of slip mechanisms in a magnesium alloy by neutron diffraction and modeling," *Scripta Materialia*, 48(8) (2003), 1003-1008.
8. A. Akhtar, and E. Teghtsoonian, "Solid solution strengthening of magnesium single crystals—II the effect of solute on the ease of prismatic slip," *Acta Metallurgica*, 17(11) (1969), 1351-1356.
9. A. Akhtar, and E. Teghtsoonian, "Solid solution strengthening of magnesium single crystals—I alloying behaviour in basal slip," *Acta Metallurgica*, 17(11) (1969),1339-1349.
10. A. H. Blake, and C. H. Cáceres, "Solid-solution hardening and softening in Mg–Zn alloys," *Materials Science and Engineering: A*, 483 (2008), 161-163.
11. N. Stanford, and M. R. Barnett, "Solute strengthening of prismatic slip, basal slip and twinning in Mg and Mg–Zn binary alloys," *International Journal of Plasticity*, 47 (2013), 165-181.
12. C. H. Cáceres, and A. Blake, "The strength of concentrated Mg–Zn solid solutions," *Physica Status Solidi A*, 194(1) (2002), 147-158.
13. H. R. Wenk, L. Lutterotti, and S. Vogel, "Texture analysis with the new HIPPO TOF diffractometer," *Nuclear Instruments and Methods in Physics Research Section A: Accelerators, Spectrometers, Detectors and Associated Equipment*, 515(3) (2003), 575-588.
14. M. A. M. Bourke, D. C. Dunand, and E. Ustundag, "SMARTS–a spectrometer for strain measurement in engineering materials," *Applied Physics A*, 74 (2002), S1707-S1709.
15. B. Clausen, *SMARTSware Manual* (Los Alamos, NM: The Regents of the University of California, 2003), 1–22.
16. R. B Von Dreele, "Quantitative Texture Analysis by Rietveld Refinement, " *J. Applied Crystallography*, 30 (4) (1997), 517–25.
17. S. R. Agnew, et al., "In situ neutron diffraction and polycrystal plasticity modeling of a Mg–Y–Nd–Zr alloy: Effects of precipitation on individual deformation mechanisms," *Acta Materialia*, 61(10) (2013), 3769-3780.
18. J. Wang, I. J. Beyerlein, and C. N. Tomé, "An atomic and probabilistic perspective on twin nucleation in Mg," *Scripta Materialia*, 63(7) (2010), 741-746.
19. B. Clausen, et al., "Reorientation and stress relaxation due to twinning: modeling and experimental characterization for Mg," *Acta Materialia*, 56(11) (2008), 2456-2468.
20. B. Raeisinia, S. R. Agnew, and A. Akhtar, "Incorporation of solid solution alloying effects into polycrystal modeling of Mg alloys," *Metallurgical and Materials Transactions A*, 42A (2011), 1418-1430.
21. B. Raeisinia and S. R. Agnew, "Using polycrystal plasticity modeling to determine the effects of grain size and solid solution additions on individual deformation mechanisms in cast Mg alloys," *Scripta Materialia*, 63(7) (2010), 731-736